HEAVY ATOM TUNNELING IN RING-OPENING REACTIONS

A COMPUTATIONAL EXPLORATION

An Undergraduate Research Scholars Thesis

by

MOLLY HUFF

Submitted to the Undergraduate Research Scholars program
Texas A&M University
in partial fulfillment of the requirements for the designation as an

UNDERGRADUATE RESEARCH SCHOLAR

Approved by
Research Advisor: Dr. Daniel Singleton

May 2016

Major: Chemistry

TABLE OF CONTENTS

ABSTRACT

Heavy-atom Tunneling in Ring-Opening Pericyclic Reactions –
An Experimental and Computational Exploration

Molly Huff
Department of Chemistry
Texas A&M University

Research Advisor: Dr. Daniel Singleton
Department of Chemistry

Though ubiquitous in everyday organic reactions, the phenomenon of tunneling must often be corrected for, and the elusive and subtle nature of its appearance in experimental studies allows it to be a continued interest for computational and organic chemists alike. Tunneling is the result of quantum mechanical principles that allow molecules to essentially "skip" their transition state and go straight to products. Heavy-atom tunneling, specifically of carbon, can have a significant effect on the rate of a reaction for certain temperatures, as evidenced by discrepancies in predicted and observed kinetic isotope effects. This thesis aims to study a reaction that is largely affected by heavy- atom tunneling and to the general features of organic reactions heavily influenced by tunneling using density functional theory computations. Oxetene was chosen as a model system because of the strained nature of its four-atom ring structure, lending itself to a tight transition state and high probability of significant heavy atom tunneling. A similar system where each hydrogen is replaced by a methyl group was also studied to determine the effect of substituent effects on potential KIEs. Significant tunneling, even at room temperatures, was calculated for both of these systems. Further experimental evidence will be gathered to further corroborate the importance of tunneling in such reactions. Because little experimental evidence

is known for this effect, though its presence is certain, the search for a concrete way to identify and predict its importance across a diverse array of organic reactions is helpful in modeling these systems.

DEDICATION

This thesis is dedicated to my family. Without them, I would not know Jesus, who has given me the knowledge and ability to carry out this project.

ACKNOWLEDGMENTS

Dr. Daniel Singleton has been absolutely a critical resource for this thesis. Without his insight, advice, and willingness to teach me new skills with patience, this project would not have been possible. A special thanks to all of the Singleton group members who also helped me incredibly along the way. I would also like to acknowledge the Texas A&M University Honors staff for their help and input. Lastly, I would like to thank Dr. Bergbreiter, who encouraged me to apply to write the thesis in the first place.

NOMENCLATURE

KIE	Kinetic Isotope Effect
QMT	Quantum Mechanical Tunneling
NMR	Nuclear Magnetic Resonance
CVT	Canonical Variational Transition State Theory
SCT	Small-Curvature Tunneling
MEP	Minimum Energy Path
PE	Potential Energy
SM	Starting Material
Prod	Product
TS	Transition State
TST	Transition State Theory

CHAPTER I

INTRODUCTION

Every chemical reaction is affected by tunneling, although the phenomenon has garnered significant attention when discussed in scientific papers. Usually tunneling occurs with hydrogen since it can occur more readily with smaller atoms. The Bell Equation, postulated by R.P. Bell to quantify the extend of tunneling in a reaction, is a correction factor Q added to the traditional Arrhenius equation in the following way:

(1) $k = QAe^{-E/RT}$

where

(2) $Q = \frac{e^{\propto}}{\beta - \propto}(\beta e^{-\propto} - \propto e^{-\beta})$ and

(3) $\propto = \frac{E}{RT}$

(4) $\beta = 2a\pi^2(2mE)^{1/2}/h$

and E is the activation energy, R is the ideal gas constant, T is temperature, m is mass, and h is Planck's constant. However, reactions that display measurable effects of tunneling from heavier atoms, such as carbon, are garnering attention in the literature. Theoretically, every reaction also has heavy-atom tunneling; it is simply much harder to observe experimentally as it is simply less prominent than hydrogen tunneling. [1]

Tunneling accounts for the excess rate of a reaction as compared to what computational models of traditional Transition State Theory (TST) would predict. It occurs when a molecule does not go through its transition state during a reaction, but "tunnels" through the energetic barrier to the product structure. Certain reactions show a much higher rate acceleration, indicating the greater effect of tunneling. This leads to unexpectedly large KIEs, temperature independence at low temperatures on the rate, and unusual A factors and activation energy (E) values. Usually this is evidenced merely by computational studies, and experimental evidence is sparse and therefore highly desirable. [2,3]

Dr. Singleton's group has demonstrated, experimentally through monitoring the kinetic isotope effect, the ability to detect significant heavy-atom tunneling independently of computed rates based on a radical ring-opening reaction[4] and more recently the Roush allylboration of aldehydes[5]. The next goal is to discover, by studying a simple representative molecule, what causes this effect to be more pronounced than would otherwise be predicted. The molecule that will be studied herein is oxetene, which is a four membered ring containing one oxygen and a C-C double bond opposite, shown in Figure 1.

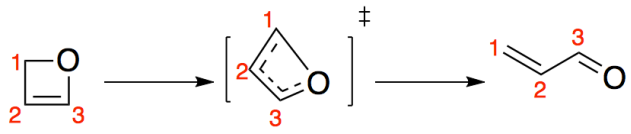

Figure 1. Oxetene (parent oxete) ring opening reaction.

This unstable molecule rapidly undergoes a semipericyclic ring opening reaction to form prop-2-en-1-al[6] and the close proximity of each atom in the transition state of the reaction further alludes to the possibility of carbon tunneling. For a simple comparison, the tetramethyl-substituted analog of the parent oxete will also be analyzed computationally to determine the effect of substituents on the extent of tunneling in the ring-opening.

Knowing the extent of tunneling, and of which carbon atom it can be attributed to, can enhance our understanding of the reaction's mechanism; organic synthesis, enzymatic studies, and even drug development are based on a detailed understanding of a reaction's mechanism and would benefit from such discovery. By experimentally synthesizing oxetene and determining the rates and kinetic isotope effect of its ring opening reaction at several temperatures, this model system can give insight into when heavy atom tunneling can significantly affect the rates of reactions. Computationally, the expected rates of reaction and kinetic isotope effects will be quantified with both tunneling corrected and non-tunneling corrected calculations. The difference in these data sets, and the differences as compared to the experimentally determined data, will give insight into how much heavy atom tunneling is present in oxetene ring openings (and presumably other similar systems).

CHAPTER II

METHODS

3-Bromo-2-(allyloxy)propanol (1)

NBS (3.56g, 20 mmol) was added to a magnetically stirred solution of allyl alcohol (6 mL) [safety: lachrymator] in 10 mL of dichloromethane (DCM) and was stirred for 12 hours at room temperature. After dilution with DCM (100 mL), the mixture was washed with 10%NaOH (aq) (3x25 mL) followed by brine, and dried over anhydrous powdered sodium sulfate. The solvent was then removed *in vacuo*. **1** was then purified with distillation under a vacuum.

3-Allyloxyoxetane

Aqueous NaOH (5g NaOH in 10 mLwater) was added to the oil of **1**. The well-stirred mixture was heated to 100-110^{o}C. The reaction is complete after approximately 15 minutes. The mixture was diluted about three times with water to dissolve the salt. The layers were separated and extracted with DCM six times. The solvent was then removed *in vacuo*.

3-Propenoxyoxetane

This compound will be synthesized next according to the Wajtowic procedure.

Ring-opening reaction computations

All reactant, product, and transition state structures were optimized using M06/6-31+G** level of theory. This was chosen after consideration of several different basis sets and methods with this level producing accurate and reproducible energy differences for the potential energy

surfaces. Rates were calculated using both transition-state theory (TST) and Canonical variational transition-state theory (CVT) with the inclusion of tunneling by using the small-curvature tunneling (SCT) approximation. Rate calculations were carried out on a M06/6-31+G** potential energy surface which used GAUSSRATE[7] to interface between POLYRATE[8] and Gaussian09[9] using the ADA supercomputing cluster at Texas A&M University.

CHAPTER III

RESULTS

Experimental results for the KIE in the parent system have not yet been obtained. The molecule has not been fully synthesized and yields of the performed reactions have not been quantified.

After carrying out single point energy calculations using 13 different methods and basis sets, Table 1 shows the calculated potential energy differences for the parent oxete system. Potential energies (PE) for the starting material (SM) and product (Prod) were obtained after normal optimization, and transition state (TS) points were obtained with an ultrafine integration parameter. All methods used a 6-31+G** basis set unless otherwise indicated.

Table 1. Single point energies of parent oxete with different levels of theory and basis sets.

Method	SM PE	TS PE	Activation Energy	Prod PE	Energy of reaction
M062X	-191.7920031	-191.7419399	31.4	-191.8302751	-24.0
m06-2x/6-311+G(2d,p)	-191.8433323	-191.7937956	31.1	-191.8830572	-24.9
CC-PVDZ	-191.356336	-191.3139385	26.6	-191.4044958	-30.2
AUG-CC-PVDZ	-191.3959142	-191.3561111	25.0	-191.441336	-28.5
CC-PVTZ	-191.5514659	-191.507247	27.7	-191.5940651	-26.7
AUG-CC-PVTZ	-191.566387	-191.5228269	27.3	-191.6076319	-25.9
CC-PVQZ	-191.6090403	-191.5647413	27.8	-191.6507931	-26.2
AUG-CC-PVQZ	-191.6148297	-191.570746	27.7	-191.6560283	-25.9
B3LYP	-191.8811622	-191.8414919	24.9	-191.9262487	-28.3
M06	-191.687739	-191.646266	26.0	-191.728733	-25.7
M11	-191.7725909	-191.7240769	30.4	-191.8109141	-24.0
wB97XD	-191.8151076	-191.7687421	29.1	-191.8550379	-25.1
PBE1PBE	-191.6593111	-191.613475	28.8	-191.6960915	-23.1

By comparing the highest level of theory, AUG-CC-PVQZ, with the other levels, it was determined that the best cost effective yet accurate method is an M06 level with 6-31+G** basis set. This was then used for subsequently reported energies and POLYRATE calculations.

Optimized structures for the starting material, transition state, and product of the oxetene and tetramethyl oxetene are shown in Figure 2.

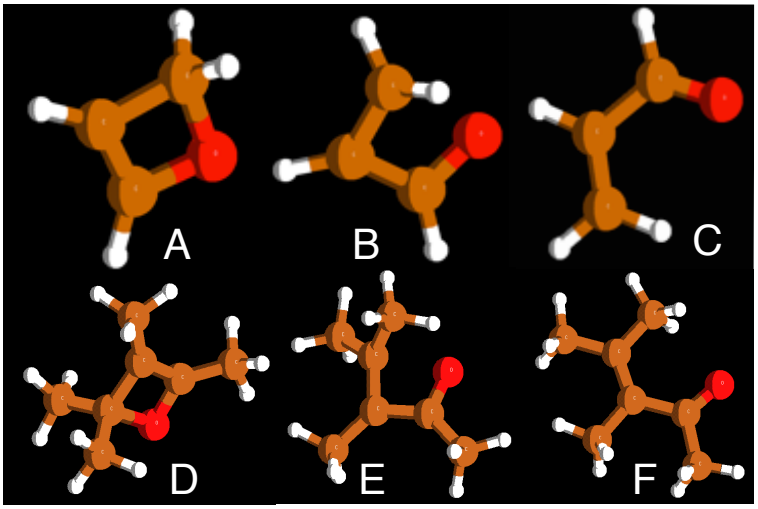

Figure 2. Optimized geometric structures of A. oxetene reactant; B. oxetene transition state; C. oxetene product prop-2-en-al; D. tetramethyl oxetene reactant; E. tetramethyl oxetene transition state; F. tetramethyl oxetene product 3,4-dimethyl-2-pentan-3-ene-one.

The rates in Table 2 were obtained for the ring-opening of the parent oxete at five representative temperatures using traditional TST calculations and using the CVT level of theory with the SCT approximation to take possible tunneling into account.

Table 2. ^{12}C rates for oxetene. All rates are in units s^{-1}.

T(K)	CVT	CVT/SCT
195.15	3.39E-17	8.61E-16
273.15	9.94E-09	2.95E-08
298.15	6.04E-07	1.45E-06
340.15	1.56E-04	2.95E-04
400	5.77E-02	8.99E-02

A similar comparison for the tetramethyl oxetene was computed and results are shown in Table 3.

Table 3. ^{12}C rates for tetramethyl oxetene. All rates are in units s^{-1}.

T(K)	TST	CVT/SCT
195.15	3.45E-25	7.04E-25
273.15	5.40E-17	7.52E-17
298.15	2.93E-15	3.84E-15
340.15	6.55E-13	8.00E-13
400	2.13E-10	2.44E-10

The rates for the tetramethyl ring opening are obviously much slower than that of the parent oxete, which is expected since along the reaction path, many more atoms must move in the tetramethyl molecule than the unsubstituted oxete.

The KIEs for each system were computed first at five representative temperatures and then at many temperatures to create an Arrhenius plot. The KIEs are largest at lower temperatures, so for the most meaningful comparison, the KIEs for each ring atom at -78^{o}C are reported for both

the parent and tetramethyl oxetes in Table 4. Atoms are labeled according to the designations in Figure 1.

Table 4. KIEs for each ring atom at -78 ^{o}C.

		TST	CVT/SCT			TST	CVT/SCT
Parent Oxete	13C1	1.05	1.26	Tetramethyl Oxete	13C1	1.06	1.08
	13C2	1.01	1.04		13C2	1.02	1.02
	13C3	1.00	1.03		13C3	1.00	1.01
	18O	1.06	1.31		18O	1.08	1.12

Again, as expected, the KIEs for the parent oxete are much higher than in the tetramethyl oxete. In addition to computing the KIEs to compare different atoms within the same molecule, information can be gained from isolating the atom with the largest KIE and comparing how the KIE changes with changing temperature. Subsequent temperatures were calculated and rates determined for the parent oxete with no heavy isotopes, and for the parent oxete with a carbon-13 at the one position which showed the highest KIE value. The results of these data are shown in Figure 3. This plots the natural log of the rate of ring-opening versus 1/T for temperatures from 30K – 400K using values obtained from CVT/SCT calculations.

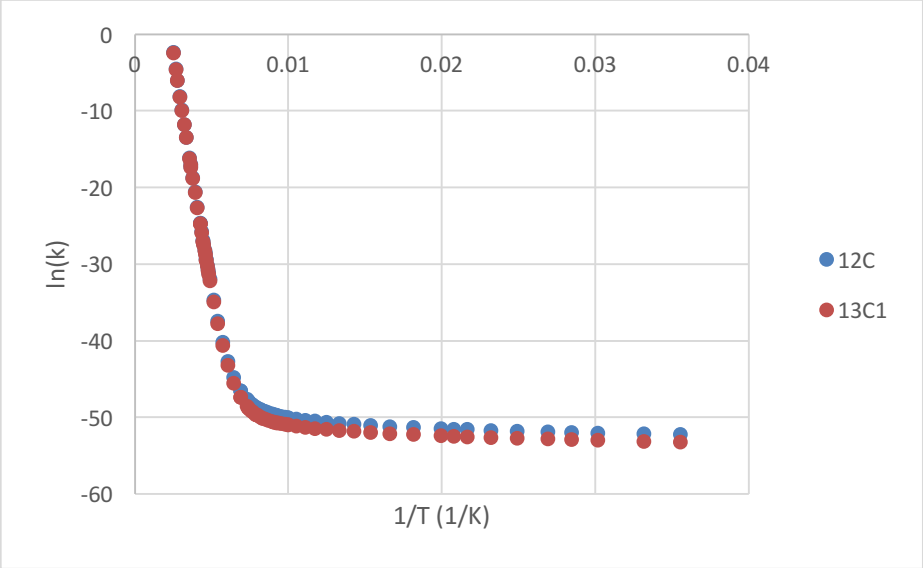

Figure 3. Arrhenius plot of rates of parent oxete reaction using CVT/SCT. Curvature at low temperatures indicates a high incidence of tunneling affecting the rate.

To understand the difference in rate data using CVT (like TST) versus CVT/SCT, the natural log of the KIE can be plotted against 1/T. Figure 4 then arranges the preceding data, plus rate data obtained from CVT, into an Arrhenius plot, which displays ln(KIE) versus 1/T for the same range. This is only the KIE for the first carbon atom, which shows the largest KIE.

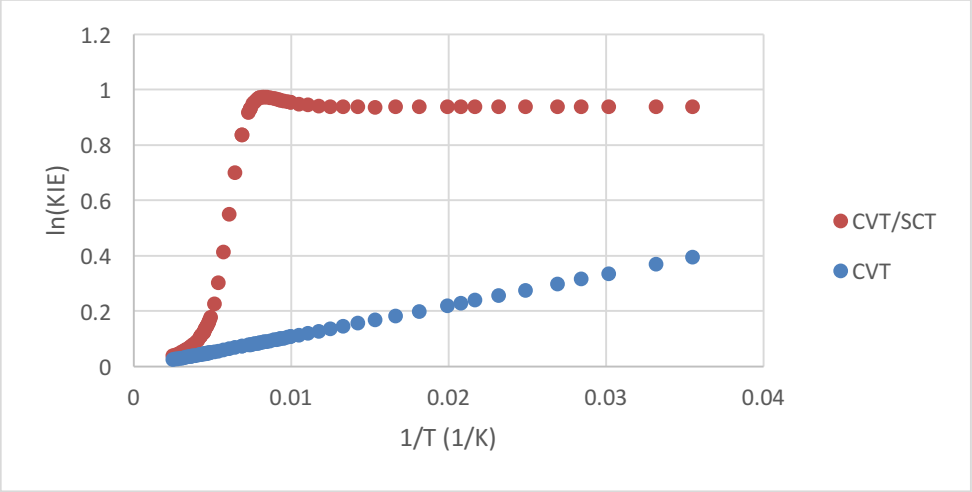

Figure 4. Arrhenius plot at C1 for CVT and CVT/SCT rate data. The large effect of temperature on the KIE at low temperatures indicates tunneling creates the large KIE disparity between these calculation methods.

A similar graph is obtained when plotting the light and heavy isotope data for the oxygen in the ring, as shown in Figure 5.

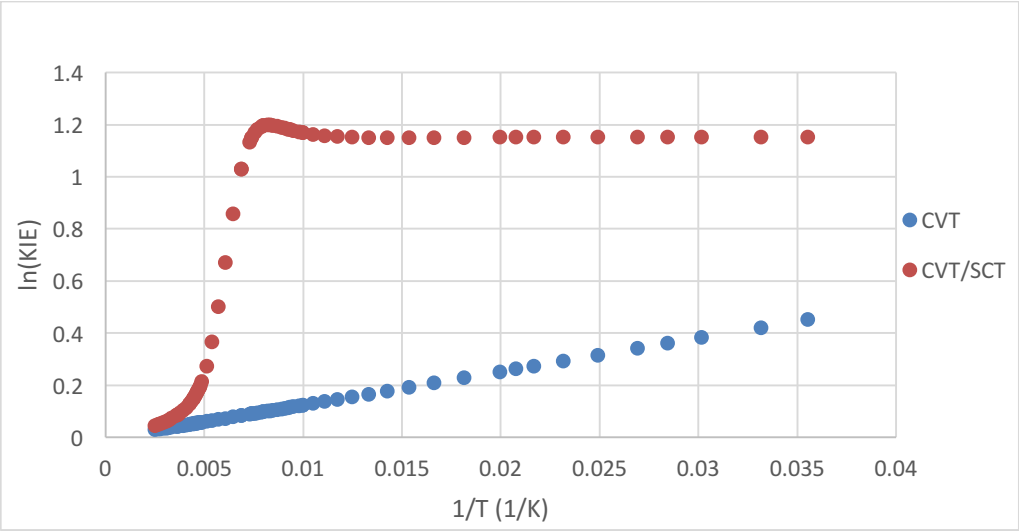

Figure 5. Comparison of CVT versus CVT/SCT methods for oxygen in the parent oxete. Again, similar tunneling effects in the oxygen are shown in large KIE disparities.

Temperature studies with the tetramethyl system were not carried out but a similar trend is expected for both the carbon and oxygen KIEs. The Arrhenius plots for both the oxygen and the carbon in the parent system show a strange “hill” around 125K. This is not normal for such plots, which typically level out without reaching a technical maximum. The presence of this maximum indicates a possible lack of numerical convergence in KIEs due to too large of a step size being used in the calculations. Computations with half the step size as used in the graphs are currently being run to see if this maximum disappears.

CHAPTER IV

CONCLUSION

The rates based on TST for the ring opening of the parent oxete system are noticeably slower, nearly 2.4 times less at room temperature, and most noticeably different as the temperatures dip below 220K. At such low temperatures, it is a quantum mechanical phenomenon that tunneling will account for an increasing amount of the rate. Usually, though, the rates are not enhanced this much. The large disparity for CVT versus CVT/SCT shown in the Arrhenius plots for the parent system (Figures 4 and 5) clearly illustrate the essential nature of a tunneling factor when considering similar reactions.

It was expected that the tetramethyl substituted oxete would have slower rates of reaction, and the computations confirm this hypothesis. Because of the slower rate of reaction and heavier nature of moving "parts" in the molecule during the ring opening, the substitution of a carbon-13 on only one carbon in the system causes a much smaller difference in the rate, since in reality the whole substituted branch of the molecule is moving during the transition state for this system, whereas in the parent oxete, only two hydrogens move with the carbon involved in bond breaking, making a carbon-13 substitution much more substantial to the reduced mass effect on the rate.

Appendix A shows more detailed computational results for both systems; molecular geometries are available upon request.

In further studies to continue into the summer, calculations with smaller step sizes will be carried out to confirm or deny the presence of an actual maximum in the Arrhenius plots of these species. If the hill persists, the physical meaning is presently unknown and will have to be carefully considered and contemplated. Also, experimental KIEs for the parent system will be carried out for at least four temperatures to confirm the existence of the abnormally high KIEs as well as deviation from the TST or CVT KIE predictions along the temperature curve.

Tunneling, though present in every chemical reaction, has herein been seen as especially important in the ring opening reaction of two different oxete compounds. These results will further be compared to other types of ring opening reactions and will undoubtedly show that strain-relieving ring-opening reactions are especially prone to heavy-atom tunneling, which was the original hypothesis for this thesis. The methods used in this study, as well as the addition of experimental KIE data, are the best known for such a study and have yielded accurate and reproducible results.

REFERENCES

(1) Bell, R. P.: *The Tunnel Effect in Chemistry*; 1 ed.; University Press: Cambridge, 1980.

(2) Gonzalez-James, O. M.; Singleton, D. A. Isotope Effect, Mechanism, and Origin of Catalysis in the Decarboxylation of Mandelylthiamin. *Journal of the American Chemical Society* **2010**, *132*, 6896-+.

(3) Meyer, M. P.; DelMonte, A. J.; Singleton, D. A. Reinvestigation of the isotope effects for the Claisen and aromatic Claisen rearrangements: The nature of the Claisen transition states. *Journal of the American Chemical Society* **1999**, *121*, 10865-10874.

(4) Gonzalez-James, O. M.; Zhang, X.; Datta, A.; Hrovat, D. A.; Borden, W. T.; Singleton, D. A. Experimental Evidence for Heavy-Atom Tunneling in the Ring-Opening of Cyclopropylcarbinyl Radical from Intramolecular C-12/C-13 Kinetic Isotope Effects. *Journal of the American Chemical Society* **2010**, *132*, 12548-12549.

(5) Vetticatt, M. J.; Singleton, D. A. Isotope Effects and Heavy-Atom Tunneling in the Roush Allylboration of Aldehydes. *Organic Letters* **2012**, *14*, 2370-2373.

(6) Jayaprakash, S.; Jeevanandam, J.; Subramani, K. Ab initio Molecular orbital and density functional studies on the ring-opening reaction of oxetene. *Journal of Molecular Modeling* **2014**, *20*, 5.

(7) Zheng, J. Z., S.; Corchado, J. C.; Chuang, Y. -Y.; Coitino, E. L.; Ellingson, B. A.; Truhlar, D. G.: Gaussrate. 2009-A ed.; University of Minnesota: Minneapolis, MN, 2010.

(8) Zheng, J. e. a.: POLYRATE. 2010 ed.; Univeristy of Minnesota: Minneapolis, MN, 2010.

(9) Frisch, J. J. e. a.: Gaussian 09. revision A.02 ed.; Gaussian, Inc: Wallingford, CT, 2009.

APPENDIX A

The following tables contain all pertinent computational data.

Table 5. Parent oxete energies.

Parent oxete	Method	POT (kcal/mol)	ΔU (kcal/mol)	EtZPE	ΔEtZPE (kcal/mol)	ENT	ΔH (kcal/mol)	G	ΔG(kcal/mol)	S(cal/mol-K)	ΔS (kcal/mol)
SM	M06-2X	-191.79200		-191.728448		-191.723955		-191.753797		62.808	
TS		-191.7419399	31.4	-191.680644	30.0	-191.676209	30.0	-191.706108	29.9	62.927	0.07
Prod		-191.8302751	-24.0	-191.768269	-25.0	-191.762933	-24.5	-191.794787	-25.7	67.043	2.66
SM	M06	-191.687739		-191.691325		-191.686795		-191.716685		62.908	
TS		-191.646266	26.0	-191.649834	26.0	-191.645322	26.0	-191.675335	25.9	63.167	0.16
Prod		-191.728733	-25.7	-191.733154	-26.2	-191.727789	-25.7	-191.759 67	-27.0	67.099	2.63

Table 6. Tetramethyl oxete energies.

Tetramethyl Oxete	Method	POT (kcal/mol)	EtZPE	ΔEtZPE (kcal/mol)	Enthalpy	ΔENT (kcal/mol)	Gibb's Free Energy	ΔG (kcal/mol)	S (cal/mol-K)	ΔS (kcal/mol)
SM	M06-2X	115.619	-348.829567		-348.819673		-348.862552		90.247	
TS		114.506	-348.781575	30.11541193	-348.770894	30.60926151	-348.815747	29.37055875	94.401	2.606672386
Prod		114.909	-348.856629	-16.981649	-348.846976	-17.132878	-348.89000	-17.220729	90.541	0.184488
SM	M06	114.125	-348.749074		-348.739134		-348.782031		90.283	
TS		112.967	-348.709551	24.80103821	-348.698812	25.3024179	-348.743675	24.0687352	94.421	2.596632242

Prod		114.476	-348.776608	-17.27783281	-348.766585	-17.22574956	-348.809914	-17.49683345	91.194	0.571660699

Table 7. ^{12}C rates and KIEs in parent oxete.

T(K)	TST	CVT/SCT
195.15	3.39E-17	8.61E-16
273.15	9.94E-09	2.95E-08
298.15	6.04E-07	1.45E-06
340.15	1.56E-04	2.95E-04
400	5.77E-02	8.99E-02

Table 8. ^{13}C1 rates and KIEs in parent oxete.

T(K)	TST	CVT/SCT	TST KIE	CVT KIE
195.15	3.21E-17	6.86E-16	1.05	1.26
273.15	9.58E-09	2.74E-08	1.04	1.08
298.15	5.84E-07	1.36E-06	1.03	1.06
340.15	1.51E-04	2.81E-04	1.03	1.05
400	5.62E-02	8.66E-02	1.03	1.04

Table 9. ^{13}C2 rates and KIEs in parent oxete.

T(K)	TST	CVT/SCT	TST KIE	CVT KIE
195.15	3.35E-17	8.31E-16	1.01	1.04
273.15	9.87E-09	2.91E-08	1.01	1.01
298.15	6.00E-07	1.43E-06	1.01	1.01
340.15	1.55E-04	2.92E-04	1.01	1.01
400	5.74E-02	8.92E-02	1.01	1.01

Table 10. ^{13}C3 rates and KIEs in parent oxete.

T(K)	TST	CVT/SCT	TST KIE	CVT KIE
195.15	3.38E-17	8.35E-16	1.00	1.03
273.15	9.91E-09	2.93E-08	1.00	1.01
298.15	6.02E-07	1.44E-06	1.00	1.01
340.15	1.55E-04	2.93E-04	1.00	1.01
400	5.75E-02	8.95E-02	1.00	1.01

Table 11. ^{18}O rates and KIEs in parent oxete.

T(K)	TST	CVT/SCT	TST KIE	CVT KIE
195.15	3.19E-17	6.55E-16	1.06	1.31
273.15	9.53E-09	2.71E-08	1.04	1.09
298.15	5.81E-07	1.34E-06	1.04	1.08
340.15	1.50E-04	2.79E-04	1.03	1.06
400	5.60E-02	8.60E-02	1.03	1.05

Table 12. ^{12}C rates and KIEs in tetramethyl oxete.

T(K)	TST	CVT/SCT
195.15	3.45E-25	7.04E-25
273.15	5.40E-17	7.52E-17
298.15	2.93E-15	3.84E-15
340.15	6.55E-13	8.00E-13
400	2.13E-10	2.44E-10

Table 13. ^{13}C1 rates and KIEs in tetramethyl oxete.

T(K)	TST	CVT/SCT	TST KIE	CVT KIE
195.15	3.26E-25	6.50E-25	1.06	1.08
273.15	5.18E-17	7.15E-17	1.04	1.05
298.15	2.82E-15	3.67E-15	1.04	1.05
340.15	6.33E-13	7.70E-13	1.03	1.04
400	2.07E-10	2.37E-10	1.03	1.03

Table 14. ^{13}C2 rates and KIEs in tetramethyl oxete.

T(K)	TST	CVT/SCT	TST KIE	CVT KIE
195.15	3.38E-25	6.87E-25	1.02	1.02
273.15	5.32E-17	7.40E-17	1.02	1.02
298.15	2.89E-15	3.78E-15	1.01	1.01
340.15	6.47E-13	7.90E-13	1.01	1.01
400.15	2.11E-10	2.42E-10	1.01	1.01

Table 15. ^{13}C2 rates and KIEs in tetramethyl oxete.

T(K)	TST	CVT/SCT	TST KIE	CVT KIE
195.15	3.44E-25	6.99E-25	1.00	1.01
273.15	5.39E-17	7.48E-17	1.00	1.00
298.15	2.92E-15	3.82E-15	1.00	1.00
340.15	6.53E-13	7.96E-13	1.00	1.00
400	2.13E-10	2.43E-10	1.00	1.00

Table 16. ^{18}O rates and KIEs in tetramethyl oxete.

T(K)	TST	CVT/SCT	TST KIE	CVT KIE
195.15	3.20E-25	6.28E-25	1.08	1.12
273.15	5.12E-17	7.01E-17	1.05	1.07
298.15	2.79E-15	3.60E-15	1.05	1.06
340.15	6.27E-13	7.58E-13	1.04	1.05
400	2.05E-10	2.34E-10	1.04	1.05